

## Stomatal Ultrastructure, Molecular Phylogeny, and Description of *Parasitodiplogaster laevigata* n. sp. (Nematoda: Diplogastridae), a Parasite of Fig Wasps

ROBIN M. GIBLIN-DAVIS,<sup>1</sup> WEIMIN YE,<sup>1,2</sup> NATSUMI KANZAKI,<sup>1</sup> DONNA WILLIAMS,<sup>3</sup> KRISTALYNNE MORRIS,<sup>2</sup>  
W. KELLEY THOMAS<sup>2</sup>

**Abstract:** *Parasitodiplogaster* comprises a potentially large radiation of nematode species that appear to be parasitically bound to their Agaonid fig wasp hosts, which are mutualistically associated in the syconia (figs) of the diverse plant genus *Ficus*. *Parasitodiplogaster laevigata* n. sp. is described and illustrated as an associate of the fig wasp, *Pegoscapus* sp. from *Ficus laevigata* from southern Florida. It is the first species of *Parasitodiplogaster* reported from North America and is closest to *P. trigonema* from *F. trigonata* from Panama. *Parasitodiplogaster laevigata* n. sp. can be differentiated from all described species of *Parasitodiplogaster* based on stomatal morphology (presence of a large dorsal and a right subventral tooth) in the adults of both sexes, molecular comparisons of two expansion segments (D2,D3) of the large subunit (LSU) rRNA gene, and fig-fig wasp host affinities. The ultrastructure of *P. laevigata* n. sp. was elucidated using TEM and SEM for comparisons with other species of *Parasitodiplogaster*. The stoma of *P. laevigata* n. sp. possesses a nonsegmented cheilostomal ring that connects to the longitudinal body musculature per- and interradially, a claw-like dorsal tooth, a right subventral tooth, and telostegostomatal apodemes arising from the dorsal side of each subventral sector. The unification of the pro-, meso-, and metastegostom with the gymnostom in *P. laevigata* n. sp. and further simplification in other described species may be due to derived adaptations associated with the internal parasitism of fig wasps.

**Key words:** Agaonidae, buccal capsule, *Ficus*, fig wasp, Hymenoptera, LSU rRNA, molecular phylogeny, morphology, nematode, parasitism, Diplogastridae, *Parasitodiplogaster laevigata* n. sp., *Pegoscapus* sp., stoma, taxonomy.

*Parasitodiplogaster laevigata* n. sp. (Nematoda: Diplogastridae) was recovered as dauer (infective) juveniles from the hemocoel of newly emerged adult females of the fig wasp *Pegoscapus* sp. (Agaonidae) and lumen of phase D syconia (figs) of *Ficus laevigata* Vahl. (*F. citrifolia* Miller sensu DeWolf) from southern Florida (Giblin-Davis et al., 1992, 1995). It is carried by female fig wasps to a new phase B syconium, where a fig wasp host pollinates and oviposits into available female florets. The female fig wasp dies inside the syconium after oviposition. The nematodes greatly increase in size as they molt and develop into fourth-stage (J4) pre-adults inside the hemocoel of their host and emerge from the wasp cadaver to finish development to adults, mate, and lay eggs giving rise to dauer juveniles. These dauer juveniles are infective to the next generation of female fig wasps as they emerge from their floret galls (Giblin-Davis et al., 1995).

There are 11 described species of *Parasitodiplogaster* that parasitize fig wasps from figs in Panama and Africa (Poinar, 1979; Poinar and Herre, 1991). Parasitism is

rare in the Diplogastridae, which are mostly omnivorous (predatory, bacterial, and/or fungal feeders) and free-living or phoretically associated with insects (Poinar, 1979; Luong et al., 1999; Fürst von Lieven and Sudhaus, 2000; Sudhaus and Fürst von Lieven, 2003). Thus, parasitism in the genus *Parasitodiplogaster* appears to be an innovation derived from free-living phoretic ancestors (Giblin-Davis et al., 2004). There is evidence from Dominican fossil amber (lower Miocene to Upper Eocene) that the association between *Parasitodiplogaster* and fig wasps is at least 19 to 25 million years old (Herre, 1995), suggesting an ancient radiation that may have developed early in the evolution of the pollination mutualism between fig wasps and figs (Giblin-Davis et al., 2004).

There are more than 700 species of *Ficus* in the world (Berg, 1989). Most species of fig wasps that are associated with species of *Ficus* from the Neotropics (140 species) and Africa (105 species) are hypothesized to harbor a unique species of *Parasitodiplogaster* (Giblin-Davis et al., 2004). Recent studies by Molbo et al. (2003) suggest that there may be more than one cryptic species of fig wasp for each species of *Ficus*, leading to the possibility of more than one species of *Parasitodiplogaster* for some species of *Ficus*.

Stomatal features have been used in generating a phylogenetic tree with molecular data of some nematode groups (Baldwin et al., 1997a,b). However, relatively little work has been done on the stoma or the phylogeny of the Diplogastridae (Baldwin et al., 1997b; Fürst von Lieven and Sudhaus, 2000; Fürst von Lieven, 2002, 2003; Sudhaus and Fürst von Lieven, 2003). In the generic diagnosis of *Parasitodiplogaster*, the stoma is described as a variably shaped cylinder that is reduced to distinct in stature, without an apparent glottoid apparatus (Poinar and Herre, 1991; but see Fürst von

Received for publication 7 October 2005.

<sup>1</sup> Fort Lauderdale Research and Education Center and Department of Entomology and Nematology, University of Florida/IFAS, 3205 College Ave., Fort Lauderdale, FL 33314-7799.

<sup>2</sup> Hubbard Center for Genome Studies, University of New Hampshire, 35 Colovos Rd., Durham, NH 03824.

<sup>3</sup> Department of Microbiology and Cell Science, University of Florida/IFAS, Bldg. 981, Rm. 1012, PO Box 110700, Gainesville, FL 32611-0700.

The authors thank Barbara J. Center, Nicole DeCrappeo, E. Allen Herre, Linda Frisse, James G. Baldwin, Henry Aldrich, and Claudia Vanderbilt for technical assistance and suggestions, and Alex Fürst von Lieven and an anonymous reviewer for helpful suggestions concerning the manuscript. This study was supported by the National Science Foundation (NSF) Tree of Life project (DEB 0228692) and a USDA Special Grant in Tropical and Subtropical Agriculture CRSR-99-34135-8478.

E-mail: giblin@ufl.edu

This paper was edited by Zafar A. Handoo.

TABLE 1. *Parasitodiplogaster* species and outgroup (*Koerneria* sp.) samples used for DNA sequencing.

Nematode species	Locality	Host	Sample No.	GenBank accession number
<i>P. citrinema</i>	Barro Colorado Isl., Panama	<i>Ficus citrifolia</i> (sensu DeWolfe)	235	AY840555
<i>P. laevigata</i> n. sp.	Palm Dr., Florida City, FL	<i>Ficus laevigata</i>	237	AY840556
<i>P. laevigata</i> n. sp.	Palm Dr., Florida City, FL	<i>Ficus laevigata</i>	245	AY840557
<i>P. laevigata</i> n. sp.	Palm Dr., Florida City, FL	<i>Ficus laevigata</i>	363	AY840558
<i>P. maxinema</i>	Barro Colorado Isl., Panama	<i>Ficus maxima</i>	236	AY840559
<i>P. popenema</i>	Barro Colorado Isl., Panama	<i>Ficus popenoei</i>	252	AY840560
<i>P. sp. ex. F. turbinata</i>	Barro Colorado Isl., Panama	<i>Ficus turbinata</i>	239	AY840561
<i>P. trigonema</i>	Barro Colorado Isl., Panama	<i>Ficus trigonata</i>	240	AY840562
<i>Koerneria</i> sp.	Lake Saranac, NY	<i>Andrena allegheniensis</i>	228	AY840563

Lieven and Sudhaus, 2000, for discussion on the presence of a glottoid apparatus vs. “bulges” in the Diplogastridae). The morphology of the stoma of nominal species of *Parasitodiplogaster* is poorly understood and has been described as “small,” “longer than wide,” or “distinct” (Poinar, 1979; Poinar and Herre, 1991). We have examined material that we collected from the type localities of several described species of *Parasitodiplogaster* for molecular analysis and concur that the stoma appears to be structurally simple as described by Poinar and Herre (1991). We know from other species of Diplogastridae that the buccal capsule/cavity is complicated to interpret (Baldwin et al., 1997b; Fürst von

Lieven and Sudhaus, 2000; Fürst von Lieven, 2002, 2003) and that the parasitic habit of *Parasitodiplogaster* could have led to structural simplification or amalgamation that would make homology difficult to discover without ultrastructural observations.

An evolutionary framework is necessary to understand this genus and its relationship to other diplogastrids and for the designation and verification of new species. Although morphology, fig and fig wasp host associations and life history will all prove useful, gene sequences provide an independent and alternative data set for phylogenetic inferences. Thus, in addition to the ultrastructural (scanning electron microscopic [SEM]

TABLE 2. Morphometrics of male holotype and female allotype in glycerol and 10 male and female specimens each of *Parasitodiplogaster laevigata* n. sp. in temporary water mounts (measurements in micrometers [ $\mu\text{m}$ ] unless otherwise stated).

Measurement or ratio	Holotype (male)	Water mounts (males)	Allotype (female)	Water mounts (females)
n	1	10	1	10
Length (mm) (mean $\pm$ S.D.; Range)	1.95	1.88 $\pm$ 0.42 (1.27–2.67)	2.46	1.98 $\pm$ 0.37 (1.35–2.76)
Body width (at vulva for females) (males = GBW; females = VBW)	79	84.5 $\pm$ 17.3 (64.7–116.2)	118	112.4 $\pm$ 20.5 (92.6–164.7)
Esophagus length	151	170.1 $\pm$ 14.7 (151.5–200.0)	150	166.2 $\pm$ 11.3 (144.1–179.4)
Anterior esophagus length	80	90.4 $\pm$ 5.4 (79.4–95.6)	80	92.1 $\pm$ 6.0 (80.9–98.5)
Posterior esophagus length	71	80.9 $\pm$ 11.9 (66.2–104.4)	70	74.4 $\pm$ 5.7 (63.2–80.9)
Posterior/anterior esophagus ratio	0.9	0.9 $\pm$ 0.1 (0.7–1.1)	0.9	0.8 $\pm$ 0.1 (0.8–0.9)
Spicule length	36	32.8 $\pm$ 4.1 (23.5–37.8)	—	—
Spicule width	7	6.3 $\pm$ 1.2 (4.4–7.4)	—	—
Vulva-to-anus distance (VA)	—	—	1050	812.6 $\pm$ 133.5 (550.0–988.2)
Anal body width (ABW)	47	52.6 $\pm$ 11.1 (41.2–70.6)	41	40.6 $\pm$ 5.6 (32.4–47.1)
Tail length	109	101.8 $\pm$ 19.7 (75.0–130.9)	119	100.2 $\pm$ 7.9 (88.2–111.8)
a	24.7	22.3 $\pm$ 2.0 (18.0–25.1)	20.8	17.7 $\pm$ 2.2 (13.8–21.2)
b	12.1	11.0 $\pm$ 2.0 (8.2–15.3)	15.9	11.9 $\pm$ 1.9 (9.4–15.9)
c	17.9	18.7 $\pm$ 3.5 (15.9–27.4)	20.7	18.9 $\pm$ 1.6 (15.4–20.4)
V (%)	—	—	48.4	52.5 $\pm$ 3.1 (46.6–57.9)



FIG. 1. Drawings of adults and juveniles of *Parasitodiplogaster laevigata* n. sp. in lateral view. A) Female. B) Male. C) Dauer (infective) juvenile. D) Second-stage juvenile.

and transmission electron microscopic [TEM]) observations and taxonomic description of *Parasitodiplogaster laevigata* n. sp., this paper reports molecular phylogenetic comparisons of two expansion segments (D2,D3) of the large subunit (LSU) rRNA gene from *Parasitodiplogaster laevigata* n. sp. with several species of *Parasitodiplogaster* from Panama.

#### MATERIALS AND METHODS

Phase B and early phase C syconia of *Ficus laevigata* were intermittently collected and dissected between 1991 and 2005 from 10 trees in a disused stretch of SE Palm Drive, Florida City, FL (25.44787° N, 80.45835° W

and 25.44799° N, 80.45519° W). *Parasitodiplogaster laevigata* n. sp. adults that had exited their *Pegoscopus* sp. fig wasp host into the lumen of the sycone were hand-picked into water prior to processing for measurements, PCR amplification, fixation for type specimens, or electron microscopy.

*Measurements and type specimens:* Adults of *Parasitodiplogaster laevigata* n. sp. were collected and heat-killed for measurements in temporary water mounts, and some of these were fixed in formalin-glycerol for greater than 24 hr and processed slowly into glycerol before making permanent slides and measurements (Southey, 1970). Nematodes were drawn and measured with the aid of a camera lucida and a stage micrometer.

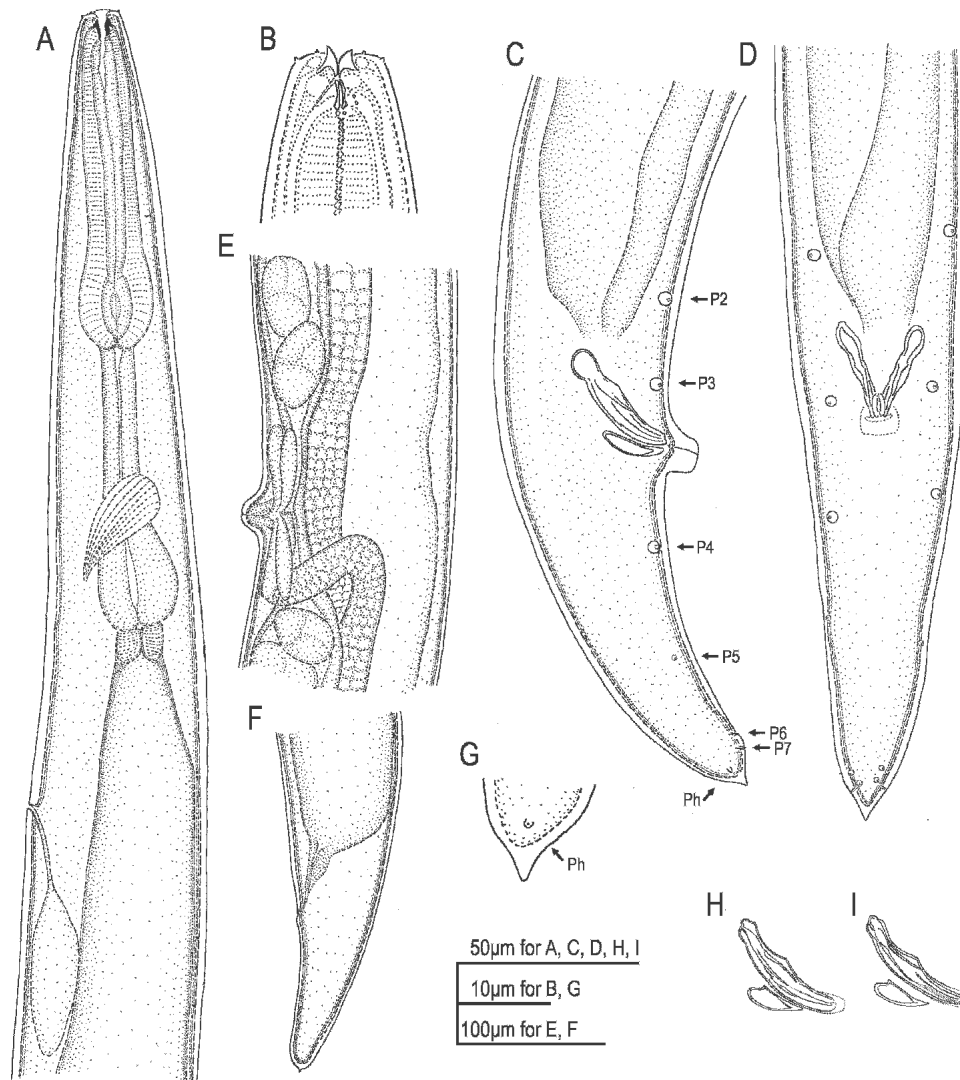


FIG. 2. Drawings of adults of *Parasitodiplogaster laevigata* n. sp. in lateral view (unless otherwise stated). A) Anterior region of female. B) Female stomatal region and anterior procorpus. C) Male tail (P2-P7 caudal papillae; Ph = phasmid). D) Male tail in ventral view. E) Female vulva and vaginal glands. F) Female tail. G) Female tail tip. H-I) Spicules and gubernaculum drawn in different focal planes.

**Scanning electron microscopy (SEM):** We examined the external morphology of adults of both sexes of *Parasitodiplogaster laevigata* n. sp. with SEM. Specimens were fixed in 3% (v/v) glutaraldehyde, post-fixed in 2% OsO<sub>4</sub> for 12 hr at 22 °C, rinsed in distilled H<sub>2</sub>O, dehydrated in a graded ethanol series, critical point dried from liquid CO<sub>2</sub>, mounted on a stub with double sticky tape, sputter-coated with 20 nm of gold-palladium, and viewed with a Hitachi (Tokyo, Japan) S-4000 Field Emission SEM at 7 kV.

**Transmission electron microscopy (TEM):** Nematode specimens were collected live into 2% formaldehyde (prepared from paraformaldehyde) and 2.5% glutaraldehyde in 0.1 M cacodylate buffer at pH 7.2 and fixed overnight at 4°C. After repeated rinsing in buffer, specimens were post-fixed in 2% OsO<sub>4</sub> in 0.1 M cacodylate buffer at pH 7.2 for 3.5 hr at 22 °C. Nematodes were rinsed in water, fixed with 1% aqueous uranyl acetate, dehydrated through 100% ethanol into 100% acetone,

and infiltrated with Spurr's epoxy resin. Blocks were sectioned on an ultra-microtome, and nearly serial sections with silver refraction (75 nm) were picked up on copper grids with a 0.35% Formvar coating reinforced with a light carbon film. Sections were post-stained with 5% aqueous uranyl acetate and lead citrate before viewing with TEM at 80 kV. One adult male nematode was transverse-sectioned and another one was sagittally-sectioned through the stoma and anterior esophagus.

**Molecular studies:** Additional *Parasitodiplogaster* species were collected as described above from *Ficus* species from the Smithsonian Tropical Research Institute, Barro Colorado Island, Republic of Panama, with assistance from E. A. Herre (Table 1). Voucher specimens were collected from the same fig as samples for amplification and sequencing attempts. Two primers D2a (ACAAGTACCGTGAGGGAAAGT) and D3b (TGC-GAAGGAACCAGCTACTA) (Nunn, 1992) were used for polymerase chain reaction (PCR) to amplify D2,D3

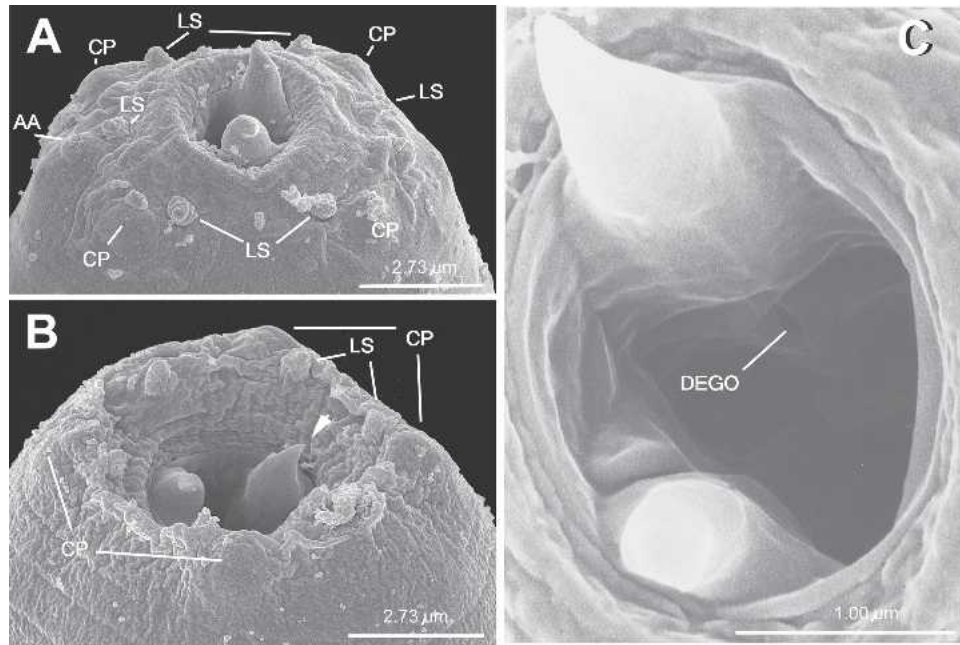


FIG. 3. SEM photomicrographs of adult heads of *Parasitodiplogaster laevigata* n. sp. A) Male with partially protracted buccal capsule. B) Female with retracted stoma. C) Higher magnification of the buccal capsule. (arrow = dorsal tooth; AA = amphidial aperture; CP = cephalic papilla dome; DEGO = dorsal esophageal gland orifice; LS = labial sensilla).

expansion segments (731 to 741 bp) of the large sub-unit of ribosomal DNA. The PCR conditions were 95°C for 5 min, 35 cycles (each cycle was 94°C, 30 sec, 55°C, 45 sec, 72°C, 2 min), then 72°C for 10 min. DNA sequencing was performed with the same primers on a CEQ 2000 DNA Analysis System (Beckman Coulter, Fullerton, CA) following manufacturer's protocols. The GenBank accession numbers for the sequences ob-

tained are presented in Table 1. DNA sequence alignment and phylogenetic analyses were as described by Ye et al. (2006) with complete references. Briefly, DNA sequences were aligned by ClustalW (Clustal Reference) using Biology Workbench (<http://workbench.sdsc.edu>, Bioinformatics and Computational Biology group, Department of Bioengineering, University of California in San Diego, CA). Phylogenetic analyses were performed in PAUP\* 4.0b10. Sites with missing data or gaps were treated as missing characters for all analyses. The maximum parsimony (MP) method was performed using a heuristic search with

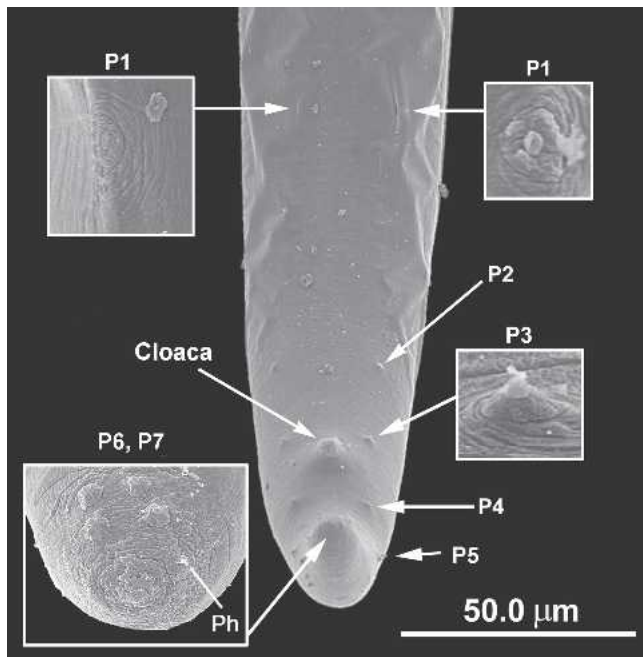


FIG. 4. SEM photomicrographs of adult male tail of *Parasitodiplogaster laevigata* n. sp. P1, P2, P3 = pre-cloacal pairs of papillae; P4–7 = post-cloacal pairs of papillae; Ph = phasmid.

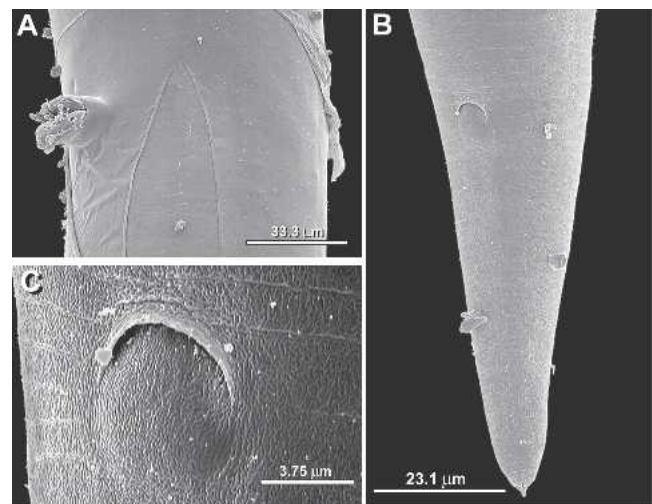


FIG. 5. SEM photomicrographs of adult female of *Parasitodiplogaster laevigata* n. sp. A) Newly molted adult ("J4-exuvia" partially attached) with protuberant vulva (lateral view). B) Tail (subventral view). C) Anus, close-up.

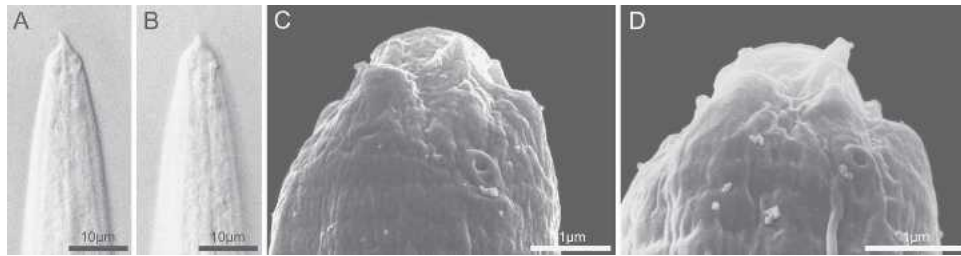


FIG. 6. Light and SEM photomicrographs of dauer juveniles of *Parasitodiplogaster laevigata* n. sp. A) Light micrograph of anterior head region showing head protuberance. B) Light micrograph of anterior head region showing amphid. C, D) SEMs of two dauer juveniles showing amphidial apertures and labial sensillae and protuberances.

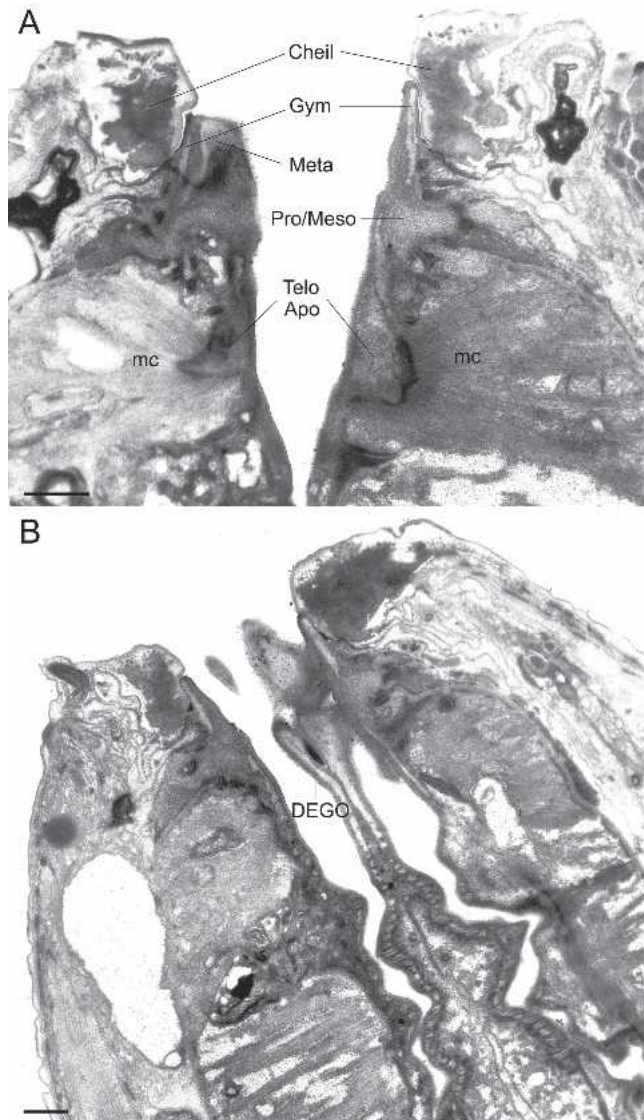


FIG. 7. TEM micrographs of the stoma of an adult male of *Parasitodiplogaster laevigata* n. sp. A) Sagittal section through the ventrosublateral aspect of the right subventral tooth (left side of photograph) and the mediolateral aspect of the left ventrosublateral sector (right side of the photograph) (Cheil = cheilostom; Gym = gymnostom; Meta = metastegostom; mc = second set of adradial muscles; Pro/Meso = Pro/Mesostegostom; Telo apo = Telostegostomatal apodeme). B) Sagittal section through the mediadorsal aspect of the dorsal tooth and the anterior triradiate branches of the procorpus showing "grinding" plates (DEGO = dorsal esophageal gland orifice) (Scale bar = 1 µm).

stepwise-addition options and neighbor-joining (NJ) using Hasegawa-Kishino-Yano 85 DNA distances. Models of evolution for likelihood analysis, as well as parameter estimates, were determined via likelihood ratio tests as

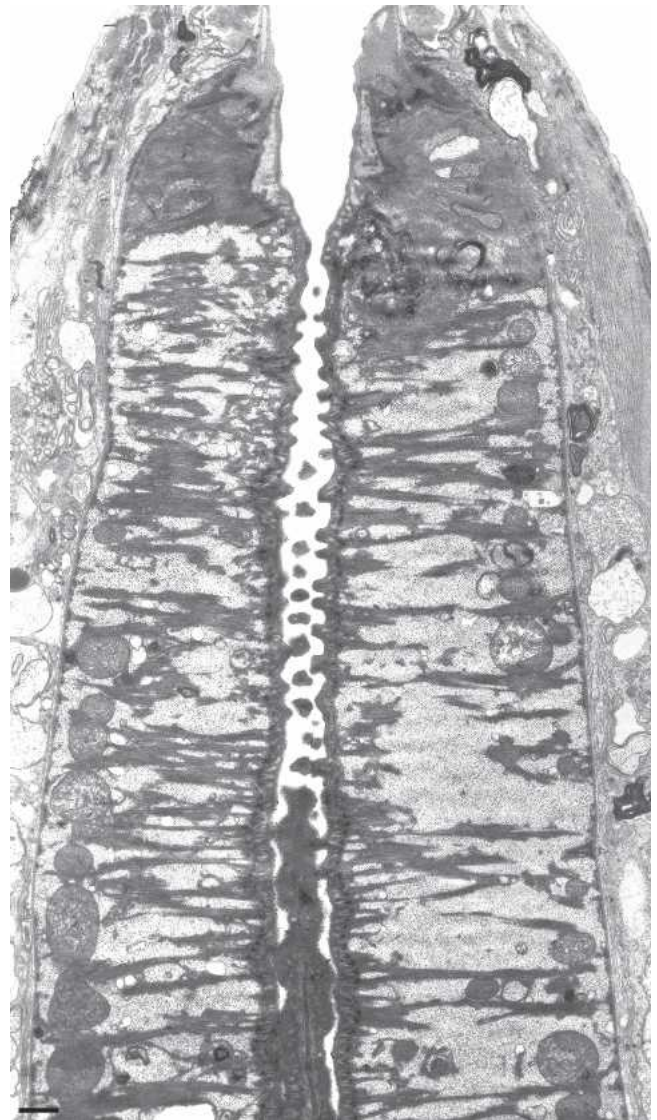


FIG. 8. TEM micrograph of a sagittal mediolateral section through the central region of the stoma and anterior procorpus of an adult male of *Parasitodiplogaster laevigata* n. sp. showing orientation and morphology of muscles, mitochondria, and overlapping sclerotized spines in the lumen of the procorpus (Scale bar = 1 µm).

implemented in Modeltest 3.06 (Posada and Crandall, 1998). The robustness of the trees was tested using the bootstrap method with all bootstrap values being based on 1,000 replicates. The aligned DNA data matrices and phylogenetic trees are available at TreeBASE (<http://www.treebase.org>, submission number: SN2592).

#### SYSTEMATICS

##### *Parasitodiplogaster laevigata* n. sp. (Figs. 1–14; Tables 1–2)

##### Description

Measurements were made of specimens in temporary water mounts and are presented in Table 2.

**Male** ( $n = 10$ ): Body large and translucent white with faint transverse cuticular striations, ventrally arcuate when killed with heat (Fig. 1B). Head without apparent lips, but with six adradial labial sensillae, one cephalic papilla dome present in each subdorsal and subventral sector (total of four), amphidial apertures circular and lateral (Fig. 3A). Lateral field not observed. Buccal capsule composed of an undivided cheilostomal ring that connects to longitudinal body musculature per- and interradially, a claw-like dorsal tooth, a right subventral tooth, and stegostomatal apodemes arising from the dorsal side of the each subventral sector that are difficult to see with light microscopy. The dorsal esophageal gland orifice exits through a stegostomatal plate below the dorsal tooth (Figs. 2B,3C,10B). Pro- and metacarpus muscular (Fig. 2A) central lumen of procorpus with small overlapping interradiial spines that point inwardly (Figs. 2B,8,11B). Terminal bulb glandular (Fig. 2A). Nerve ring (circumesophageal commissure) circumscribes isthmus just anterior to terminal bulb (Fig. 2A). Cardia present. Excretory pore located ventrally about three cardia lengths posterior to the esophago-intestinal junction. Hemizonid not observed. Gonad outstretched, almost reaching excretory pore (Fig. 1B). Tail ventrally curled; about 1.9 anal body widths long. No bursa present. Seven ventral, sub-ventral, or ventro-sublateral preanal (3) and postanal (4) pairs of papillae (according to terminology of Sudhaus and Fürst von Lieven [2003]; v1–3/v4, ad, v5–6, ph with the apparent loss of pd and one of the v5–7 triad). One pair of preanal subventral papillae (P1 = v1) at about three anal body widths anterior to cloaca (visible only with SEM), one pair of preanal subventral papillae (P2 = v2) at about one anal body width anterior to cloaca, one pair of subventral preanal papillae (P3 = v3) just anterior to cloaca, one pair of subventral postanal papillae (P4 = v4) about  $\frac{1}{2}$  anal body width posterior to cloaca, one small pair of ventrosublateral postanal papillae (P5 = ad) posterior to P4 at about 55% of the tail length behind cloaca, two ventral pairs of papillae (P6–7 = v5–6), and pore-like phasmids located laterally just be-

fore tail tip (Figs. 2C–D, 4). Spicules separate; spicule length about 33  $\mu\text{m}$ , gubernaculum about 40–50% of spicule length (Figs. 2C–D,H–I; Table 2). Tail with small mucron.

**Female** ( $n = 10$ ): Adult female cuticular features and cephalic regions (exterior and interior) similar to males (Figs. 1A,2A–B,3B). Ventrally arcuate when killed with heat (Fig. 1A). Ovaries didelphic and reflexed, eggs usually present, in single cell through gastrula stages (Fig. 1A). Vulval position at about 50% of body length (Fig. 1A; Table 2), vulva a protuberant oval pore (Figs. 1A,2E,5A), four vaginal glands present (Fig. 2E). Anus dome-shaped (Figs. 5B–C). Tail uniformly conoid with small mucron present (Figs. 2F–G,5B). Phasmids located near tail tip (Fig. 2G).

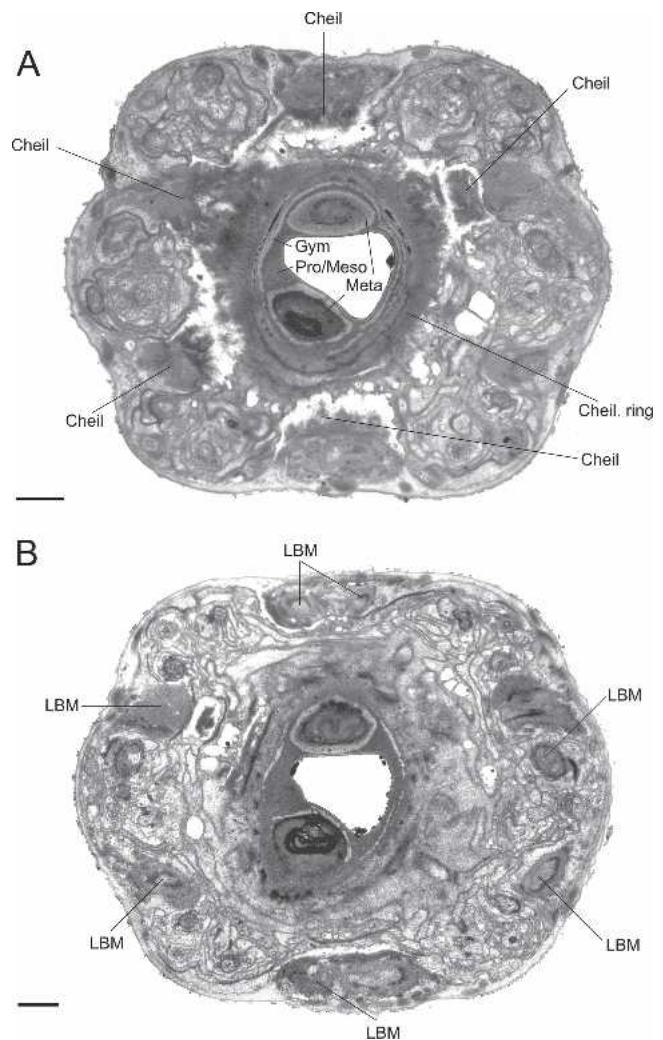


FIG. 9. TEM micrographs of the stoma of an adult male of *Parasitodiplogaster laevigata* n. sp. A) Almost transverse section through the cheilostomal ring (Cheil. ring), per- and interradial cheilostomatal connections (Cheil) to the longitudinal body musculature (LBM), and combined stegostomatal unit with gymnostom and dorsal tooth and right subventral tooth embedded in pro-/mesostegostomatal ring that is partially telescoped through the cheilostomal ring (Gym = gymnostom; Meta = metastegostom; Pro/Meso = Pro/Mesostegostom). B) Almost transverse section posterior to section A through combined stegostomatal unit showing longitudinal body muscles (LBM) (Scale bar = 1  $\mu\text{m}$ ).

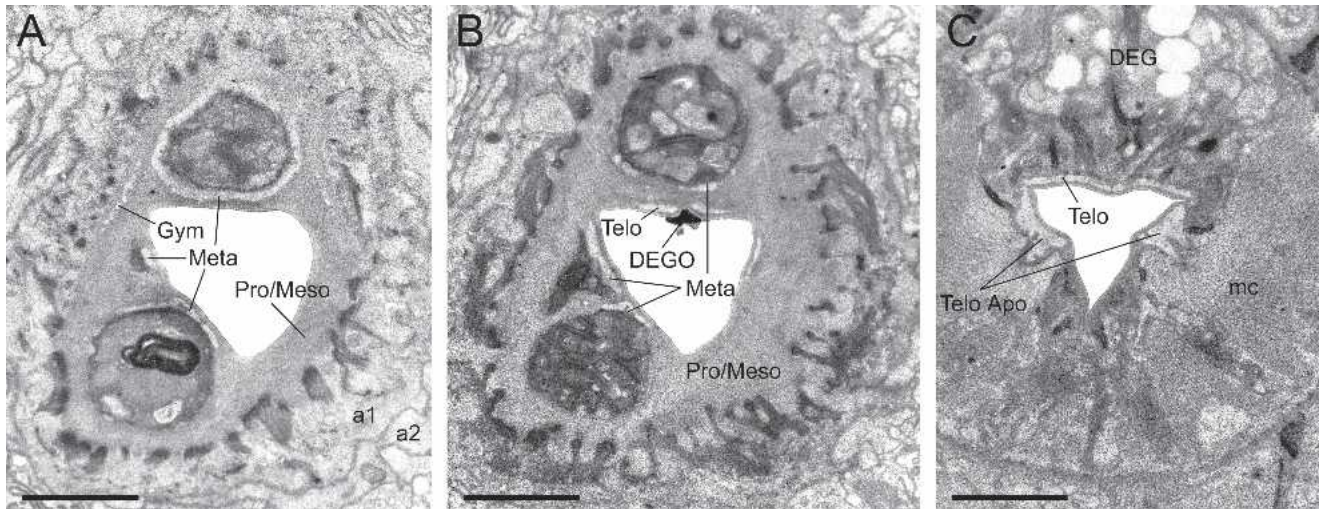


FIG. 10. TEM micrographs of the stoma of an adult male of *Parasitodiplogaster laevigata* n. sp. A) Almost transverse section through the combined stegostomatal unit (a1, a2 = arcade syncytial rings; Gym = gymnostom; Meta = metastegostom; Pro/Meso = Pro/Mesostegostom). B) Almost transverse section through the combined stegostomatal unit posterior to section A (DEGO = dorsal esophageal gland orifice; Telo = telostegostom). C) Almost transverse section through the telostegostom posterior to the section in Figure 11A (DEG = dorsal esophageal gland; mc = second set of adradial muscles; Telo Apo = telostegostomatal apodemes) (Scale bar = 1  $\mu$ m).

*Dauer juveniles from newly emerged female wasps* ( $n = 12$ ): Measurements of the dauer juveniles follow (Mean  $\pm$  SD; [range]): total body length =  $260.0 \pm 40.4$  (198.7–344.1)  $\mu$ m; esophagus length =  $100.9 \pm 14.9$  (80.8–130.0)  $\mu$ m; greatest body width =  $18.7 \pm 2.5$  (16.2–25.0)  $\mu$ m; gonad primordium length =  $9.5 \pm 1.9$  (7.5–13.3)  $\mu$ m; gonad primordium width =  $5.9 \pm 0.9$  (4.6–7.5)  $\mu$ m; tail length =  $29.5 \pm 4.8$  (21.7–35.8)  $\mu$ m; anal body width =  $10.4 \pm 0.7$  (9.2–11.7)  $\mu$ m; a =  $13.9 \pm 1.6$  (11.4–16.6); b =  $2.6 \pm 0.2$  (2.4–2.9); c =  $7.7 \pm 1.4$  (5.8–9.9); and c' ratio =  $25.0 \pm 3.8$  (19.1–31.2). Body cylindrical, tapered at both ends (Fig. 1C). Small dorsal-ventral ridge on the head appears tooth-like in dorsal or ventral view (Fig. 6), lateral tooth-like protrusion anterior to lateral labial sensilla above amphid (Fig. 6D). Circular amphids visible (Fig. 6B–D), stoma and esophagus degenerate, excretory pore at level of nerve ring, anus visible, phasmids visible about one third of the tail length from terminus, tail uniformly conoid, slightly attenuated. The second-stage instar (Fig. 1D) hatches from eggs in the fig sycone and precedes the dauer in development (Fürst von Lieven, 2005). The third instar appears to be an obligatory dauer because no further development occurs in the fig before infection of adult fig wasps. This second-stage instar has an apparently functional toothed stoma and esophagus (with an “a” ratio of about 3.4 vs. 2.4 in the dauer) (Figs. 1C–D).

*Diagnosis:* *Parasitodiplogaster laevigata* n. sp. is distinguished from all other described species of *Parasitodiplogaster* by the unique morphology of the stoma in both sexes with the possession of large dorsal and right subventral teeth, biogeography, and Agaonid and *Ficus* host range (associated with *Pegoscapus* sp. in *Ficus laevigata* in southern Florida).

*Relationships:* Based upon D2,D3 LSU sequence data

of collected *Parasitodiplogaster*, *P. laevigata* n. sp. is closest to an undescribed species of *Parasitodiplogaster* ex *Ficus turbinata* and to *P. trigonema* from *F. trigonata* from Panama (Figs. 14–15). The number of nucleotide autapomorphies between *P. laevigata* n. sp. and *P. trigonema* (= 17) and *P. sp. ex Ficus turbinata* (= 14) is indicative of a large number of fixed novel differences in the concerted evolution of the D2,D3 LSU region, suggestive of separate but closely related species (Fig. 15). There is strong evidence for a clade of *Parasitodiplogaster* (*P. laevigata* n. sp., *P. sp. ex Ficus turbinata*, *P. trigonema*, *P. poppenema*, and *P. citrinema*), all collected from the genus *Ficus*, subgenus *Urostigma*, section *Americana* (100% bootstrap support with MP, NJ, and ML analyses) (Fig. 14). *Parasitodiplogaster maxinema*, which was isolated from *Ficus maxima*, a member of the *Ficus* subgenus *Pharmacosycea*, section *Pharmacosycea*, appears outside this clade, suggesting that this lineage resulted from cospeciation with its fig and fig wasp hosts, as suggested by Giblin-Davis et al. (2004). *Koerneria* sp. was chosen as an outgroup for this study because of its apparent “nearest-relative” status in preliminary D2,D3 LSU trees within the Diplogastridae (Ye et al., unpubl. data), and this was corroborated by trees from wider surveys done of the Diplogastridae and clade V representatives using near full-length sequences of LSU and SSU rRNA genes (Kiontke and Fitch, pers. comm.).

*Parasitodiplogaster laevigata* n. sp. appears morphologically closest to *P. trigonema* from *F. trigonata* from Panama. In both species, the testes is outstretched, spicules are straight with blunt tips and a distinct manubrium, the gubernaculum is straight and wedge-shaped, often with a swollen proximal end, there are three (in *Parasitodiplogaster laevigata* n. sp.) and four (in *P. trigonema*) subventral preanal papillae in series up the body

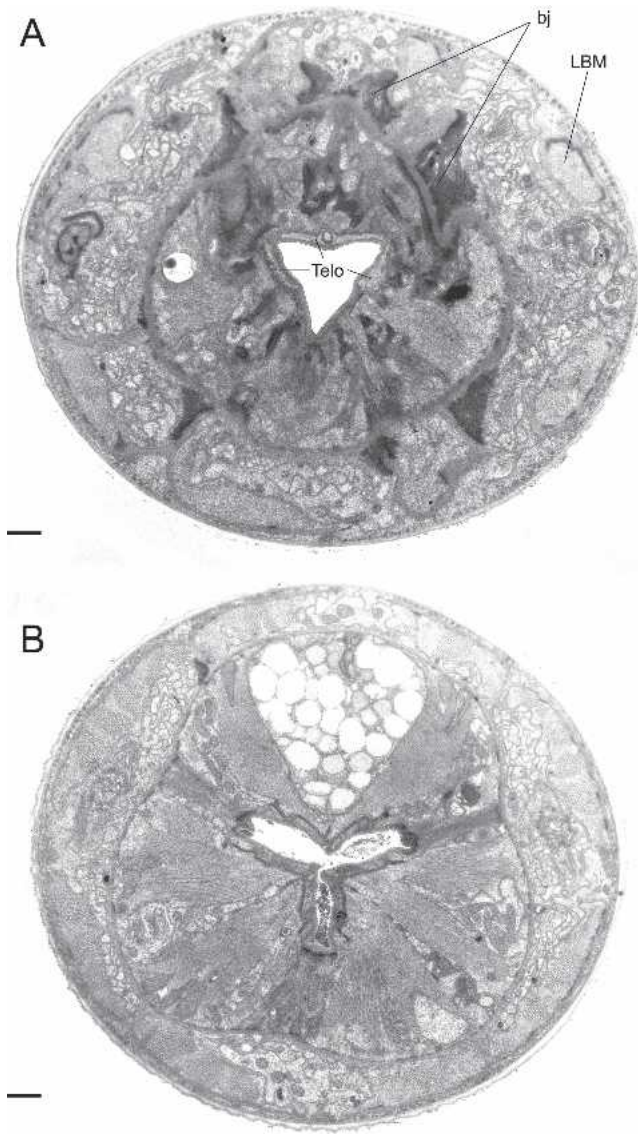


FIG. 11. TEM micrographs of the stoma of an adult male of *Parasitodiplogaster laevigata* n. sp. A) Almost transverse section through the telostegostom (= Telo) posterior to section in Fig. 10B and anterior to section in Fig. 10C showing belt junctions (=bj) that extend from the base of the pro/mesostegostomatal matrix (see Fig. 10B) and anchor the stegostomatal unit to longitudinal body muscles (LBM) and cuticle. B) Almost transverse section through the anterior portion of the procorpus revealing the triradiate lumen of the esophagus and interdigitating spines that point inwardly in the central portion of the lumen. (Scale bar = 1  $\mu$ m).

and four similarly placed pairs of postanal papillae, distinct phasmids at tail tip beyond last papilla, and the tail tip is usually mucronated. In addition, both sexes of both species have similar excretory pore positioning, posterior to the esophago-intestinal junction. Besides the difference in the number of preanal papillae in males, there are a number of significant morphological differences between these two species, including a muscular procorpus with a well-developed cardia in both sexes of *P. laevigata* n. sp. as opposed to a glandular-appearing procorpus and a weak cardia in *P. trigonema*. The structuring of the sclerotized lining of the procor-

pus into “tongue and groove” ridges and presence of small overlapping interradiial spines that point inwardly appear to represent autapomorphies in *P. laevigata* n. sp. In addition, the stoma of *P. laevigata* n. sp., which possesses a distinct dorsal and right subventral tooth, is not only distinct from *P. trigonema*, which has a small 2- $\mu$ m  $\times$  2- $\mu$ m stoma with no teeth, but from all other described species that have variably described cylinders without major teeth.

*Type host and locality:* Holotype male and allotype female of *P. laevigata* n. sp., which had recently exited their *Pegoscapus* sp. fig wasp host into the lumen of the sycone in an early phase C syconia of *F. laevigata*, were collected from Florida City, FL.

*Type designations:* Holotype male, allotype female and additional material deposited at the University of California-Riverside Nematode Collection. Paratypes (males and females same data as holotype) deposited at the University of California, Davis; USDA Nematode Collection, Beltsville, MD; and the Nematology Department, Rothamsted Experiment Station, Harpenden, Herts., United Kingdom.

*Etymology:* This species name is derived from the species name of the *Ficus* host with which the nematode is associated in southern Florida, i.e., *Ficus laevigata*.

*Ultrastructural observations and discussion:* These are the first ultrastructural observations of the stoma of *Parasitodiplogaster*, which should prove useful for understanding changes in feeding structures that have occurred in the evolution of parasitism in the Diplogastriidae. Previously used nomenclature in the ultrastructural work of the stoma of *Acrostichus halicti* by Baldwin et al. (1997b) was reconciled with the stomatal terminology of De Ley et al. (1995) for Rhabditidae and Panagrolaimidae, and Cephalobidae by Fürst von Lieven and Sudhaus (2000). In addition, they discussed their hypotheses concerning the homologization of the buccal regions of this nematode with other clade IV and V nematodes and provided some excellent light microscopic observations and drawings of a variety of stomatal structures in the Diplogastriidae that will serve as a basis for the discussion herein.

The stoma of *P. laevigata* n. sp. is composed of a short telescoping unit involving the cheilostom and a combined unit of the gymnostom and stegostom. The undivided cheilostomal ring attaches to longitudinal body musculature in the head (Figs. 9A,12) at the six perradiial and interradiial sectors (Fig. 9A). At the dorsal interradiial and the ventral perradiial (marginal) sectors, the cheilostomal ring connects to two longitudinal body muscles as opposed to the right and left subdorsal perradiial and the right and left subventral interradiial sectors, which each connect to a single longitudinal body muscle (Fig. 9B). Interestingly, J4 juveniles of *Koerneria* sp. (Strain RG20 = RGD228 in this study) have an undivided cheilostomal ring with vertical striations vs. adults, in which the cheilostom is divided into six

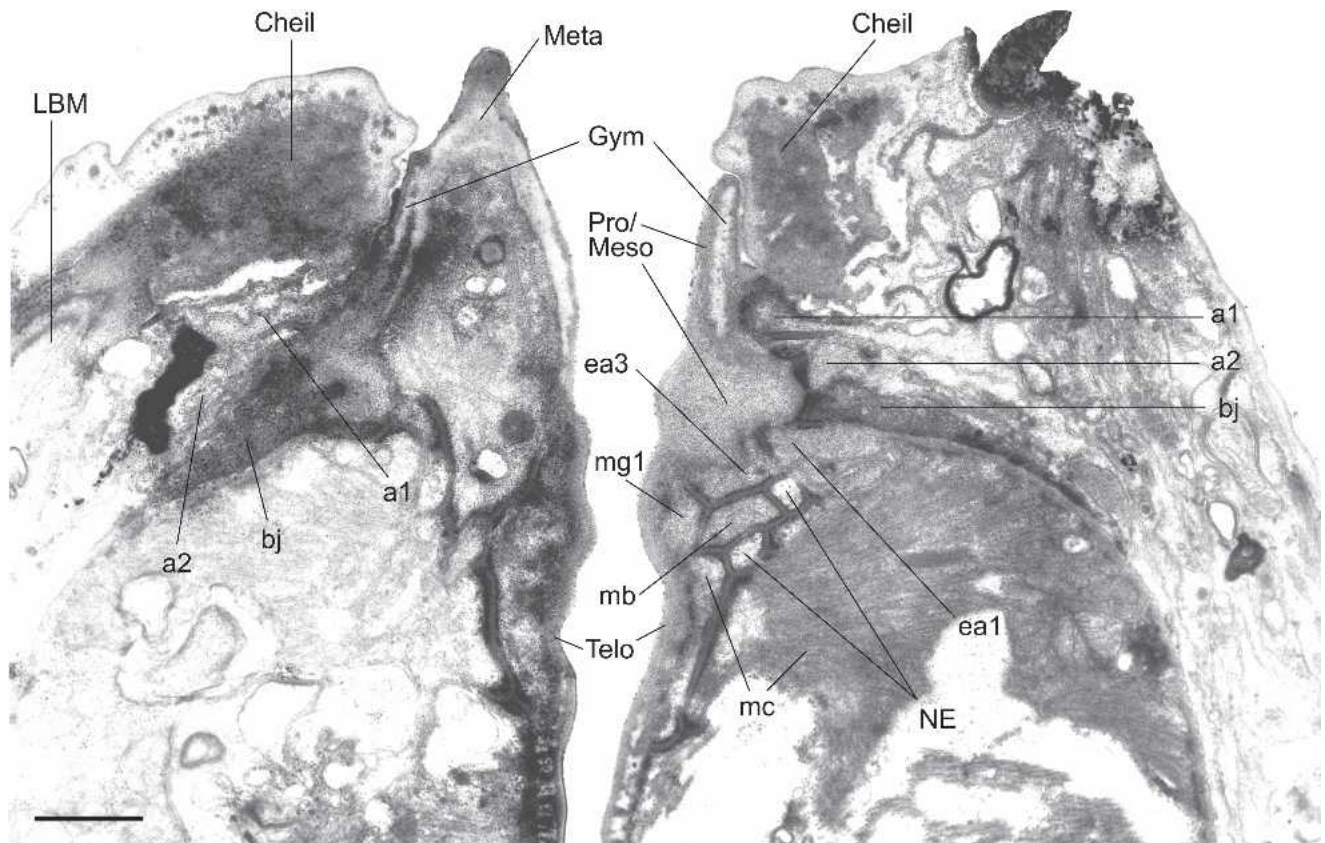


FIG. 12. TEM micrograph of an almost sagittal section through the right subventral tooth (left side of photograph) and the ventrosub-lateral aspect of the left subventral sector (right side of the photograph) of the stoma of an adult male of *Parasitodiplogaster laevigata* n. sp. (a1, a2 = arcade syncytial rings; bj = belt junction; Cheil = cheilostom; ea1 = first set of interradiial epithelial cells; ea3 = second set of interradiial epithelial cells; Gym = gymnostom; LBM = longitudinal body muscle; mb = first set of adradial muscles; mc = second set of adradial muscles; Meso = mesostegostom; Meta = metastegostom; mg1 = first set of marginal cells; NE = nerve ending; Pro = Prostegostom; Telo = Telostegostom). (Scale bar = 1  $\mu$ m).

per- and interradiial plates (Fürst von Lieven and Sudhaus, 2000). This contrasts with *A. halicti*, where the cheilostom is divided into six adradial plates (Baldwin et al., 1997b; Fürst von Lieven and Sudhaus, 2000).

The gymnostom of *P. laevigata* n. sp. is an electron lucent ring in transverse section, associated with two

rings of arcade syncytia, which is apparently fused with most of the stegostomatal components into a cohesive, non-telescoping unit (Figs. 7,9,12). The gymnostom of *P. laevigata* n. sp. appears embedded in what we are interpreting to be a matrix produced by the first and second sets of interradiial epithelial cells (ea1, ea3) (Figs. 12,13). According to Fürst von Lieven and Sudhaus (2000), this cuticular matrix, which is similar to that observed in *A. halicti*, should be homologized with a fused pro/mesostegostom which, in *C. elegans*, appears as unresolved linear stomatal components that are associated with each interradiial epithelial cell (ie1, ie2). In some sagittal sections from *P. laevigata* n. sp., a zone of demarcation between the relatively darker-staining prostegostom and the lighter-staining mesostegostom could be discerned (Figs. 12,13). However, in other sections it was not possible to separate the two zones.

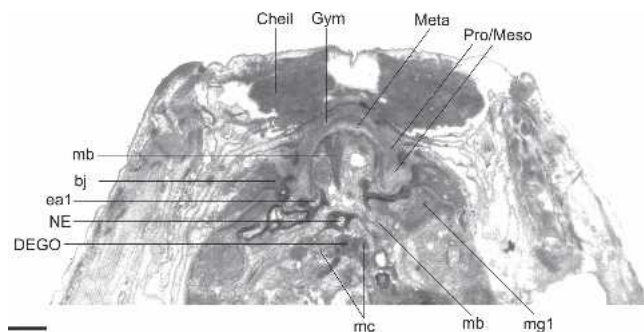


FIG. 13. TEM micrograph of an almost sagittal section through the back of the dorsal tooth in the stoma of an adult male of *Parasitodiplogaster laevigata* n. sp. (bj = belt junction; Cheil = cheilostom; DEGO = dorsal esophageal gland orifice; ea1 = first set of interradiial epithelial cells; Gym = gymnostom; mb = first set of adradial muscles; mc = second set of adradial muscles; Meso = mesostegostom; Meta = metastegostom; mg1 = first set of marginal cells; NE = nerve ending; Pro = Prostegostom). (Scale bar = 1  $\mu$ m).

Another striking feature of *P. laevigata* n. sp. is the asymmetry of the metastegostomatal teeth, apparent fusion or suspension of the metastegostomatal teeth in the pro/mesostegostomatal matrix, and significant reduction in size of the associated first set of adradial muscle cell homologs (mb). As we interpret it, the con-

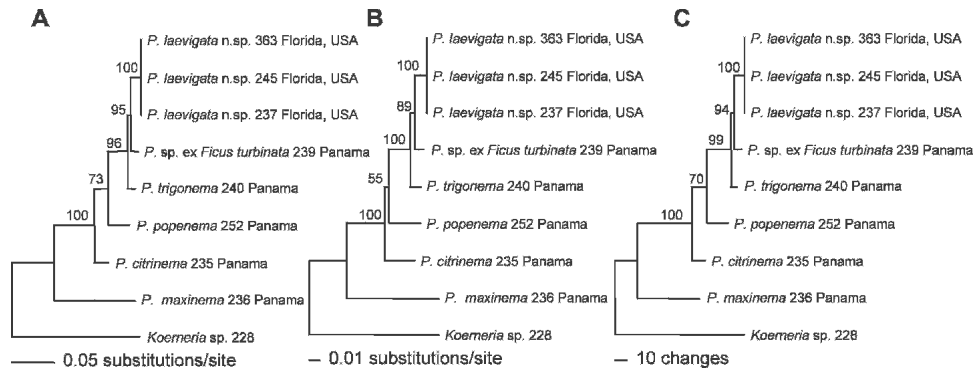


FIG. 14. Phylogenetic trees were inferred from the analyses of molecular sequence data of *Parasitodiplogaster laevigata* n. sp. and other New World Tropical species of *Parasitodiplogaster*. Sequences from the D2,D3 expansion segments of LSU (731–741 bp) were aligned and used in A) maximum likelihood (ML), B) neighbor joining (NJ), and C) maximum parsimony (MP) analyses. All bootstrap values are based on 1000 replicates.

tractile component of the first set of adradial muscle cell homologs (mb) is reduced and inside each tooth (Fig. 13). This contrasts with *Koerneria* sp., which possesses very large and longitudinally oriented adradial muscles that attach to the dorsal tooth and extend into the esophagus (Fürst von Lieven and Sudhaus, 2000). The dorsal and right subventral teeth are quite robust and claw-like in *P. laevigata* n. sp., similar to *Koerneria* sp. There is a small mediolateral projection in the right subventral sector, of apparent metastegostomatal origin, that appears to be associated with cellular components (Figs. 3C,10A,B). However, its derivation and function are unknown. If we accept that *Parasitodiplogaster* is the sister group of *Koerneria*, as the molecular data suggest, then the loss or reduction of stegostomatal armatures in all of the currently described species of *Parasitodiplogaster* becomes problematic. The dorsal and right subventral claw-like teeth in *P. laevigata* n. sp. could have evolved de novo after being lost in the stem-ancestor of *Parasitodiplogaster*, or the teeth could have been lost independently several times (Figs. 14–15). We hypothesize that when *Parasitodiplogaster* is fully characterized, it will represent a large radiation of species from the Neotropics, Africa, and other parts of the

world. Thus, interpretations of evolutionary trends must be postponed until we have characterized more species from a wider geographical sampling of species.

Fürst von Lieven and Sudhaus (2000) posit that homologization of the stoma in *C. elegans* and the Diplogastridae is aided by the presence or absence of a pair of putative proprioceptive nerve endings at the anterior and posterior midline of each subventral metastegostomatal sector and a single nerve ending in the dorsal telostegostomatal plate just above the orifice of the dorsal esophageal gland. Two nerve endings each were clearly present in *P. laevigata* n. sp. in the left subventral sector in sagittal section (Fig. 12) and the right subventral sector (not shown), and a single one was confirmed in the dorsal sector (Fig. 13), but the presence of foramina (innervated indentations in the meta- or telostegostomatal plates) were not confirmed for any of these nerve endings.

The following is our hypothesis for functionality of the stoma in *P. laevigata* n. sp. given our understanding of the ultrastructure. When the longitudinal body muscles are contracted, the oral opening is dilated and the cheilostomal ring is pulled back, allowing for the protraction of the large, claw-like metastegostomatal

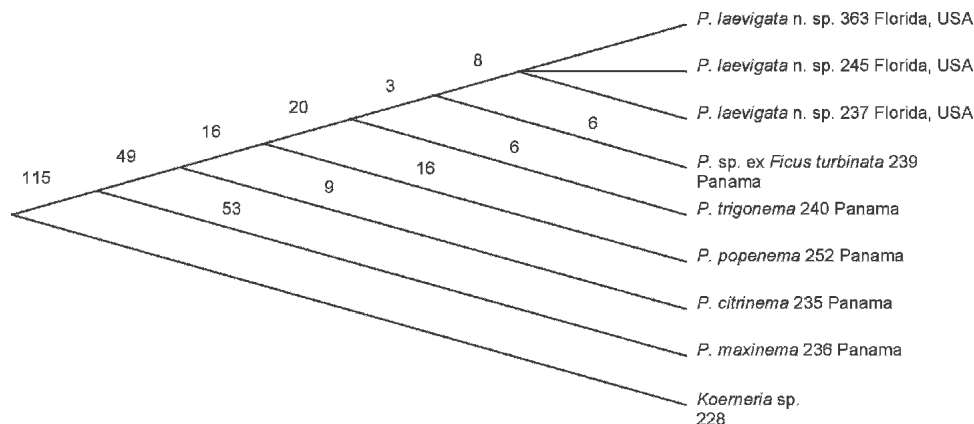


FIG. 15. Cladogram based upon the alignment of 746 characters (including gaps and insertions) from D2,D3 expansion segments of LSU. Each number represents the number of apomorphies.

dorsal and right subventral teeth slightly beyond the entrance of the mouth (Fig. 3A). When the body muscles are relaxed, the cheilostomal ring returns to its normal shape, and the belt junctions (or tendons?) connecting the pro/mesostegostom at its base (Figs. 10A,B) to larger belt junctions (or tendons?) (Fig. 11A) that connect to a framework of bands that attach to the longitudinal body muscles and cuticle hold the fused gymnostom and pro/meso and metastegostom in place, allowing for retraction of the teeth. Each tooth appears to lack the musculature that would allow independent movement.

The dorsal esophageal gland orifice exits the dorsal telostegostomatal plate into the buccal cavity. The anterior-most region of this plate is embedded in the pro/mesostegostom matrix without direct fusion to the dorsal tooth (Fig. 7B,10B) as apparently occurs in other Diplogastridae (Baldwin et al., 1997b). There is a small pair of adradial muscles that attach to this plate. In contrast, strong adradial muscles (mc) attach to the telostegostomatal apodemes that arise from the dorsal side of each subventral sector (Figs. 7A,10C) that, when contracted, may dilate the lumen of the stoma from a triangle in transverse section to a more pentagonal shape. This action could create suction or help to mix food. Fürst von Lieven and Sudhaus (2000) consider the presence of stegostomatal apodemes to be an apomorphy that helps to justify the *Koerneria* clade.

Each marginal branch of the triradiate lining of the procorpus has sclerotized, integrating "tongue and groove-like" ridges through its entire length that are visible only in sagittal view (Fig. 7B) and suggest a grinding or crushing function for the entire procorpus. Interestingly, the radial muscles of the procorpus are relatively thin and evenly distributed among large glycogen-looking reserves with mitochondria oriented mostly at the periphery and perpendicular to the lumen (Fig. 8). In addition, the dorsal and subventral interradiate aspects of the central lumen of the procorpus are equipped with small, overlapping sclerotized spines that point inwardly (Fig. 8, 11B), perhaps for further piercing or crushing of food.

Thus, although it is difficult to discern feeding habits from morphology alone, we hypothesize that the unique stomatal morphology of *P. laevigata* n. sp. may be adapted for tearing and/or hooking internal organs of its fig wasp host when its large teeth are protracted through the action of longitudinal body muscle contractions and that host tissue is pulled into the buccal cavity when longitudinal body muscles are relaxed. In the telostegostom, secretions from the dorsal esophageal gland may be added for extra-corporeal digestion, while contraction and relaxation of adradial muscles (mc) attached to the dorsal subventral telostegostomatal sectors may begin to help move tissue into the anterior procorpus for crushing and piercing by the unique sclerotized lining.

Poinar and Herre (1991) suggested that the Panama *Parasitodiplogaster* species represent a monophyletic radiation from a single stem species with a variety of stomatal and esophageal manifestations to match their ecology. Herre (1995) has argued that the expression of virulence by *Parasitodiplogaster* is correlated with its chances for horizontal or vertical transmission by the fig wasp, with virulence being expressed most in associations where the number of female foundresses per fig is high and least in associations where the number is low. Giblin-Davis et al. (1995) reported a level of about 1.5 pollinator wasp foundresses per fig for *Pegoscapus* sp. in *Ficus laevigata*, but observed that ovipositing foundresses were infested with *P. laevigata* n. sp. dauers that had not yet developed or were very small J4s, suggesting that the nematodes may delay development to reduce parasitic effects on their host until oviposition and pollination have occurred. Thus, even if the morphology of the stoma or esophagus suggests tissue destruction and potential virulence such as in *P. laevigata* n. sp., much more work is needed to confirm the expression of virulence. Poinar and Herre (1991) suggested that *Parasitodiplogaster* with small stomas, glandular esophagi, and thin-walled intestines (e.g., *P. trigonema*) may be adapted for a liquid diet as opposed to those with large stomas, muscular esophagi, and small intestinal cells with a border that may be adapted for solid food (e.g., *P. laevigata* n. sp.). These two *Parasitodiplogaster* species may be good candidates for further study because they have divergent feeding morphologies but are closely related according to male primary and secondary sexual characters and molecular phylogenetic analysis (Fig. 14).

#### LITERATURE CITED

- Baldwin, J. G., Frisse, L. M., Vida, J. T., Eddleman, C. D., and Thomas, W. K. 1997a. An evolutionary framework for the study of developmental evolution in a set of nematodes related to *Caenorhabditis elegans*. *Molecular Phylogenetics and Evolution* 8:249–259.
- Baldwin, J. G., Giblin-Davis, R. M., Eddleman, C. D., Williams, D. S., Vida, J. T., and Thomas, W. K. 1997b. Buccal capsule of *Aduncospiculum halicti* (Nemata: Diplogasterina): An ultrastructural and molecular study with implications for phylogeny. *Canadian Journal of Zoology* 33:407–423.
- Berg, C. C. 1989. Classification and distribution of *Ficus*. *Experientia* 45:357–358.
- DeLey, P., Van De Velde, M. C., Mounport, D., Baujard, P., and Coomans, A. 1995. Ultrastructure of the stoma in Cephalobidae, Panagrolaimidae, and Rhabditidae, with a proposal for a revised stoma terminology in Rhabditida (Nematoda). *Nematologica* 44:153–182.
- Fürst von Lieven, A. 2002. Functional morphology, origin, and phylogenetic implications of the feeding mechanism of *Tylopharynx foetida* (Nematoda: Diplogastrina). *Russian Journal of Nematology* 10:11–23.
- Fürst von Lieven, A. 2003. The genus *Oigolaimella* Paramonov, 1952 (Nematoda: Diplogastridae) and description of *Oigolaimella kruegeri* n. sp. and *O. ninae* n. sp. *Nematology* 5:583–600.
- Fürst von Lieven, A. 2005. The embryonic moult in diplogastrids (Nematoda) – homology of developmental stages and heterochrony as a prerequisite for morphological diversity. *Zoologischer Anzeiger* 244:79–91.

- Fürst von Lieven, A., and Sudhaus, W. 2000. Comparative and functional morphology of the buccal cavity of Diplogastrina (Nematoda) and a first outline of the phylogeny of this taxon. *Journal of Zoological Systematics and Evolutionary Research* 38:37–63.
- Giblin-Davis, R. M., Center, B. J., Nadel, H., Frank, J. H., and Ramirez, B. W. 1995. Nematodes associated with Fig wasps, *Pegoscapus* spp. (Agaonidae), and the syconia of native Floridian figs (*Ficus* spp.). *Journal of Nematology* 27:1–14.
- Giblin-Davis, R. M., Davies, K. A., Taylor, G. S., and Thomas, W. K. 2004. Entomophilic nematode models for studying biodiversity and cospeciation. Pp. 492–538 in Z. X. Chen, S. Y. Chen, and D. W. Dickson, eds. *Nematology, advances and perspectives*, vol. 1. New York: Tsinghua University Press/CABI Publishing.
- Giblin-Davis, R. M., Nadel, H., and Frank, J. H. 1992. New species of *Schistonchus* and *Parasitodiplogaster* parasitizing the fig wasp, *Pegoscapus assuetes*, in the syconia of *Ficus citrifolia*. *Journal of Nematology* 24:592.
- Herre, E. A. 1995. Factors affecting the evolution of virulence: Nematode parasites of fig wasps as a case study. *Parasitology* 111:S179–S191.
- Luong, L. T., Platzer, E. G., De Ley, P., and Thomas, W. K. 1999. Morphological, molecular, and biological characterization of *Mehdi-nema alii* (Nematoda: Diplogasterida) from the decorated cricket (*Grylloides sigillatus*). *Journal of Parasitology* 85:1053–1064.
- Molbo, D., Machado, C. A., Sevenster, J. G., Keller, L., and Herre, E. A. 2003. Cryptic species of fig-pollinating wasps: Implications for the evolution of the fig-wasp mutualism, sex allocation, and precision of adaptation. *Proceedings of the National Academy of Sciences* 100: 5867–5872.
- Nunn, G. B. 1992. Nematode molecular evolution. PhD dissertation. University of Nottingham, U.K.
- Poinar, G. O., Jr. 1979. *Parasitodiplogaster sycophilon* gen. n., sp. n. (Diplogasteridae: Nematoda), a parasite of *Elisabethiella stuckenbergi* Grandi (Agaonidae: Hymenoptera) in Rhodesia. *Proceedings of the Koninklijke Nederlandse Akademie van Wetenschappen, Series C, Biological and Medical Sciences* 82:375–381.
- Poinar, G. O., Jr., and Herre, E. A. 1991. Speciation and adaptive radiation in the fig wasp nematode *Parasitodiplogaster* (Diplogasteridae: Rhabditida) in Panama. *Revue de Nématologie* 14:361–374.
- Posada, D., and Crandall, K. A. 1998. Modeltest: Testing the model of DNA substitution. *Bioinformatics* 14:817–818.
- Southey, J. F., ed. 1970. *Laboratory methods for work with plant and soil nematodes*. London: Her Majesty's Stationery Office.
- Sudhaus, W., and Fürst von Lieven, A. 2003. A phylogenetic classification and catalogue of the Diplogasteridae (Secernetea, Nematoda). *Journal of Nematode Morphology and Systematics* 6:43–90.
- Ye, W., Giblin-Davis, R. M., Braasch, H., Morris, K., and Thomas, W. K. 2006. Phylogenetic relationships among *Bursaphelenchus* species (Nematoda: Parasitaphelenchidae) inferred from nuclear ribosomal and mitochondrial DNA sequence data. *Molecular Phylogenetics and Evolution* (In Press).